

Synthesis and antimicrobial activity of 6-sulfo-6-deoxy-D-glucosamine and its derivatives

Kornelia Skarbek ^a, Iwona Gabriel ^b, Piotr Szweda ^b, Marek Wojciechowski ^b, Muna A. Khan ^c, Boris G. Erke ^c, Sławomir Milewski ^b, Maria J. Milewska ^a

^a Department of Organic Chemistry, Gdańsk University of Technology, Gdańsk, Poland

^b Department of Pharmaceutical Technology and Biochemistry, Gdańsk University of Technology, Gdańsk, Poland

^c Department of Microbiology, Immunobiology and Genetics, Max F. Perutz Laboratories, University of Vienna, Vienna Biocenter, Vienna, Austria

Abstract

6-Sulfo-6-deoxy-D-glucosamine (GlcN6S), 6-sulfo-6-deoxy-D-glucosaminitol (ADGS) and their N-acetyl and methyl ester derivatives have been synthesized and tested as inhibitors of enzymes catalyzing re-actions of the UDP-GlcNAc pathway in bacteria and yeasts. GlcN6S and ADGS at micromolar concentrations inhibited glucosamine-6-phosphate (GlcN6P) synthase of microbial origin. The former was also inhibitory towards fungal GlcN6P N-acetyl transferase, but at millimolar concentrations. Both compounds and their N-acetyl derivatives exhibited antimicrobial *in vitro* activity, with MICs in the 0.125–2.0 mg mL⁻¹ range. Antibacterial but not antifungal activity of GlcN6S was potentiated by D-glucosamine and a synergistic antibacterial effect was observed for combination of ADGP and a dipeptide Nva-FMDP.

1. Introduction

Enzymes participating in biosynthesis of polysaccharides constituting microbial cell walls are considered promising targets for antimicrobial chemotherapy [1,2]. These include four enzymes of the cytosolic pathway leading to the ultimate formation of UDP-GlcNAc, a sugar-nucleotide precursor of chitin in fungi and peptidoglycan in bacteria. Interestingly, the fungal and bacterial versions of the pathway are somewhat different. In fungi, the four successive reactions are as follows: (a) conversion of fructose-6-P (Fru6P) into glucosamine-6-phosphate (GlcN6P); (b) acetylation of GlcN6P to GlcNAc6P; (c) isomerization of GlcNAc6P to GlcNAc1P; and (d) uridylation of GlcNAc1P to give UDP-GlcNAc [1]. In prokaryotic cells, the first and the last step are essentially the same, but GlcN6P is first isomerized to give GlcN1P, which is subsequently N-acetylated [2]. In both versions, the first committed step is catalyzed by the enzyme known under a trivial name of GlcN6P synthase. The target potential of this enzyme has been already demonstrated [3].

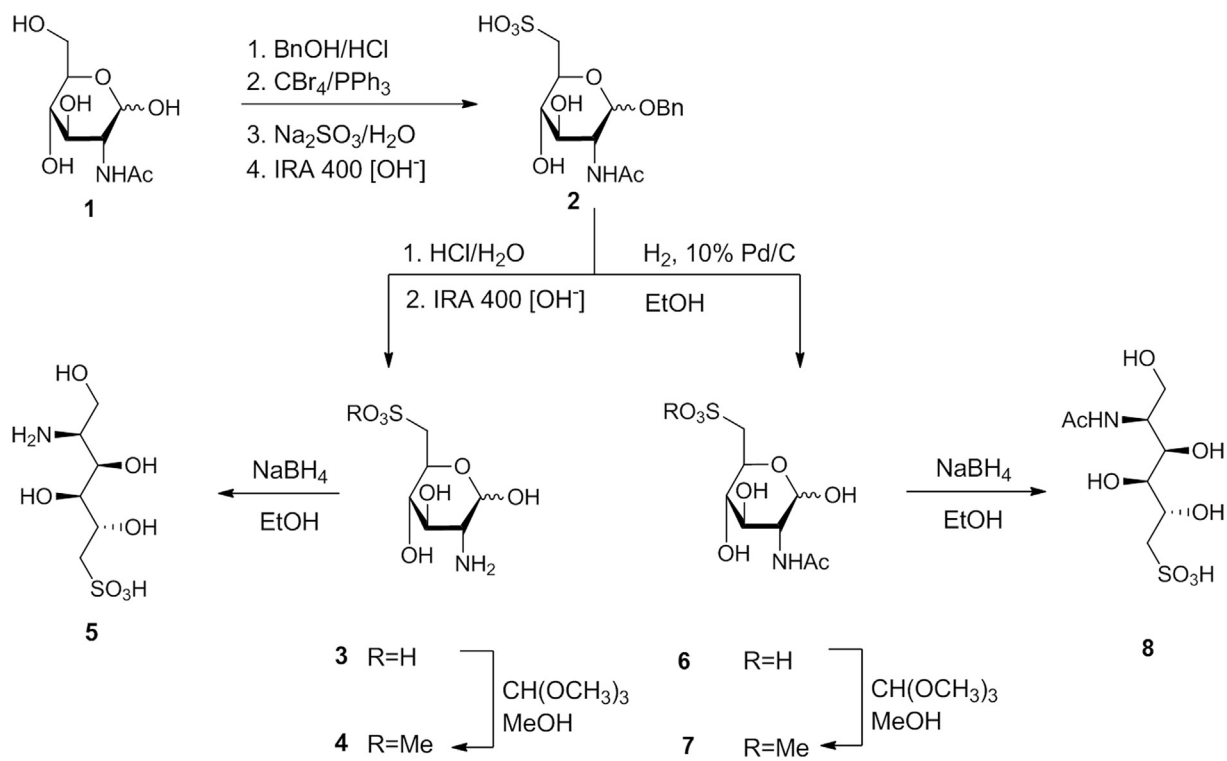
Inhibitors of GlcN6P synthase known to date are structural analogs of L-glutamine, including N³-(4-methoxyfumaryl)-L-2,3-diaminopropanoic acid (FMDP), analogs of the *cis*-enolamine transition state intermediate, including 2-amino-2-deoxy-D-glucitol-6-phosphate (ADGP) and of the reaction product, *i.e.* GlcN6P. ADGP and GlcN6P inhibit the enzyme *in vitro* but demonstrate low antimicrobial activity, due to the poor uptake by microbial cells and intracellular metabolism, including possible phosphatase-assisted dephosphorylation of both and degradation by NagB or conversion to GlcN1P by GlcN6P isomerase (GlmM) of the latter, obviously preventing access to the target enzyme [4,5]. In search for the cell penetrating and non-metabolizable inhibitors of enzymes of the UDP-GlcNAc pathway, we have synthesized 2-amino-6-sulfo-2,6-dideoxy-D-glucose (GlcN6S), its N-acetyl and methyl ester derivatives, 2-amino-2,6-dideoxy-D-glucitol-6-sulfonic acid (ADGS) and NAcADGS. One of these compounds, namely GlcN6S, was previously shown to exhibit growth inhibitory activity against some bacteria [6], other compounds are entirely novel.

2. Results

2.1. Chemistry

The synthetic strategy leading to compounds **3–8** is outlined in Scheme 1. An initial substrate was the commercially available N-

Abbreviations: cfu, colony forming units; GlcN, D-glucosamine; IPTG, isopropyl β-thiogalactoside; ISOM, isomerase domain of GlcN6P synthase; LB, Luria-Bertani; MIC, minimal inhibitory concentration; UDP-GlcNAc, uridine 5'-diphospho-N-acetyl-D-glucosamine.



Scheme 1. Synthetic strategies applied in this work. Bn, benzyl; Ph, phenyl.

acetyl-D-glucosamine **1**. Steps leading to the compound **3** were slightly modified in comparison to the method reported previously in literature [6]. After formation of the benzyl acetal of **1**, treatment with tetrabromomethane in pyridine and triphenylphosphine allowed substitution of the 6-OH group by bromine. Subsequently, the bromine was replaced by the sulfonic group derived from sodium sulfite. The acetyl and benzyl groups were removed upon treatment with hydrochloric acid, to give **3**. A selective removal of the benzyl group from **2** by hydrogenolysis in the presence of Pd/C afforded **6**. Compounds **3** and **6** were converted into their respective methyl esters **4** and **7** upon treatment with trimethoxymethane in methanol. On the other hand, reduction of **3** or **6** with sodium borohydride gave the 2-amino-2,6-dideoxy-D-glucitol-6-sulfonic acid **5** and its *N*-acetyl derivative **8**, respectively.

2.2. Antimicrobial activity

Antibacterial and antifungal activity of compounds **3–8** was determined by a serial dilution microplate method. Minimal inhibitory concentrations (MICs) determined in buffered RPMI-1640 medium (yeasts) or in Mueller-Hinton Broth (bacteria) are shown in Table 1.

Compounds **3**, **5**, **6** and **8** demonstrated moderate antifungal and antibacterial activity, with MICs in the 0.125–2.0 mg mL⁻¹ range. The aminoglucitol 6-sulfonate ADGS **5** was in most cases more active than its non-reduced cyclic counterpart, GlcN6S **3**. *N*-acetylation slightly improved antimicrobial activity of GlcN6S and ADGS (comparison of **3** and **6** and **5** and **8**, respectively). The methyl esters of GlcN6S and ADGS (compounds **4** and **7**) were inactive. No antimicrobial activity (MICs >>4.0 mg mL⁻¹) was noted for GlcN6P.

The antimicrobial activity of GlcN6S, ADGS and their *N*-acetyl derivatives was completely abolished (MIC values >>4.0 mg mL⁻¹) when growth media were supplemented with GlcNAc, 10 mg mL⁻¹. Since it is well known that GlcNAc is effectively accumulated by

Table 1
Antimicrobial *in vitro* activity of GlcN6S, ADGS and their derivatives.

Compound	MIC (mg mL ⁻¹)							
	Bacteria				Yeasts			
	SA ^a	SE	EC	PA	CAL	CG	CK	CAR
GlcN6S 3	1.0	2.0	2.0	2.0	1.0	2.0	1.0	0.5
GlcN6SME 4	>4.0	>4.0	>4.0	>4.0	>4.0	>4.0	>4.0	>4.0
ADGS 5	0.25	1.0	0.5	0.5	1.0	1.0	0.5	0.5
NAcGlcN6S 6	0.5	1.0	0.5	1.0	0.5	0.25	0.25	0.25
NAcGlcN6SME 7	>4.0	>4.0	>4.0	>4.0	>4.0	>4.0	>4.0	>4.0
NAcADGS 8	0.125	0.25	0.5	0.25	1.0	0.5	0.5	0.25

^a SA, *Staphylococcus aureus*; SE, *Staphylococcus epidermidis*; EC, *Escherichia coli*; PA, *Pseudomonas aeruginosa*; CAL, *Candida albicans*; CG, *Candida glabrata*; CK, *Candida krusei*; CAR, *Candida arborea*.

both bacterial and fungal cells and immediately phosphorylated to give GlcNAc6P, this result confirms that a molecular target for compounds **3**, **5**, **6** and **8** is an enzyme catalyzing any of the three initial steps in the UDP-GlcNAc pathway. Surprisingly, presence of GlcN potentiated an antibacterial activity of GlcN6S, while fully reversed the growth inhibitory effect of a dipeptide, Nva-FMDP. The latter is a known antimicrobial agent targeting GlcN6P synthase, *i.e.* an enzyme catalyzing the first committed step of the UDP-GlcNAc pathway [7,8]. The MIC value of compound **3** against *E. coli*, determined in the presence of GlcN, 10, mg mL⁻¹ was 4-fold lower than that of compound **3** alone (0.5 mg mL⁻¹ vs. 2.0 mg mL⁻¹, respectively). GlcN alone did not show any antibacterial activity and, on the other hand, the antifungal action of GlcN6S was not affected by GlcN.

An interesting phenomenon was a synergistic antibacterial effect of GlcN6S **3** in combination with Nva-FMDP, as shown in Fig. 1. Synergism was not observed for combination of **3** with Nva-FMDP, acting on *C. albicans* cells (not shown).

Action of **3**, **5**, **6** and **8** on *C. albicans* cells, at concentrations

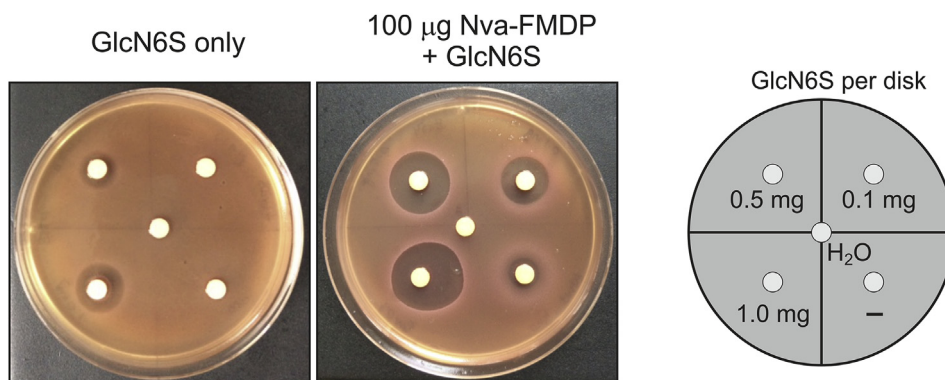


Fig. 1. Disk diffusion assay of antibacterial activity of Nva-FMDP and GlcN6S in combination against *E. coli* cells.

exceeding the respective MIC values, induced strong morphological changes, including agglutination, swelling and destruction of cell integrity. Another consequence was inhibition of septum formation, known to be composed exclusively of chitin, as documented in photos shown in Fig. 2 (cells stained with Calcofluor White for chitin).

2.3. Intracellular metabolism

Composition of the cell-free extracts prepared from the *C. albicans* cells incubated for 3 h in the presence of GlcN6SME, NAcGlcN6S, NAcGlcN6SME and NAcADGS was investigated by thin layer chromatography (TLC) analysis. In all cases the original substances could be identified in cell-free extracts, thus confirming their internalization. These studies showed that GlcN6SME **4** was not metabolized to any detectable derivative, particularly no traces of GlcN6S **3** were found in the respective cell-free extract (S12). On the other hand, this metabolite was detected in the cell-free extract of cells grown in the presence of NAcGlcN6S **6** (S12) and traces of ADGS **5** were found in the cell-free extract of cells incubated in the presence of NAcADGS **8**. Finally, the cell free extract of cells incubated in the presence of NAcGlcN6SME **7** contained traces of GlcN6SME **4** but not of GlcN6S **3**.

2.4. Enzyme inhibitory activity

All compounds were tested as inhibitors of GlcN6P synthase from *C. albicans*. Two methods of activity assay were employed: determination of GlcN6P formed (the Elson-Morgan procedure) in the case of ADGS **5** and its *N*-acetyl derivative **8** and determination of L-glutamate in the case of GlcN6S **3** and its derivatives **4**, **6** and **7**. The latter was necessary, since GlcN6S, similarly as GlcN6P, forms a purple product in the Elson-Morgan reaction.

Data presented in Table 2 show that GlcN6S **3** and ADGS **5** inhibited enzyme activity and 50% inhibition was observed at 0.08 and 0.13 mM, respectively, while 90% inhibition was noted at

Table 2
Inhibition of GlcN6P synthase by GlcN6S, ADGS and their derivatives.

Compound	IC ₅₀ (mM)	
	GFA1 (<i>C. albicans</i>)	GlmS (<i>E. coli</i>)
GlcN6S 3	0.08 ± 0.03	0.21 ± 0.08
GlcN6SME 4	>5	>5
ADGS 5	0.13 ± 0.05	0.18 ± 0.02
NAcGlcN6S 6	>5	>5
NAcGlcN6SME 7	>5	>5
NAcADGS 8	>5	>5

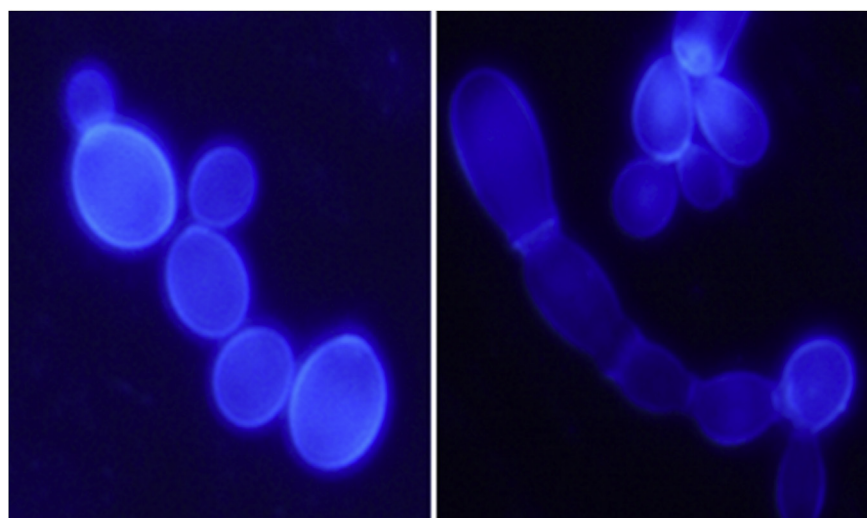


Fig. 2. Visualization of chitin biosynthesis inhibition in *C. albicans* cells. Cells were stained with Calcofluor White. Left – control; Right – cells treated with ADGS 5, 1 mg mL⁻¹ for 3 h.

0.2–0.4 mM. None of the derivatives **4**, **6**, **7** and **8** inhibited the fungal enzyme. Inhibition of bacterial GlcN6P synthase was tested in the cell-free extract of *E. coli* cells overproducing the enzyme. GlcN6S **3** and ADGS **5** inhibited this enzyme with IC_{50} values similar to those determined for the fungal GlcN6P synthase.

Compounds **3**, **4** and **6** were also tested as potential inhibitors of GlcN6P N-acetylase in *C. albicans* cell-free extract. No inhibition was noted for the ester **4** and the N-acetyl derivative **6** at concentrations <5 mM but GlcN6S **3** inhibited the enzyme with $IC_{50} = 2.85 \pm 0.23$ mM. The same compounds, as substrate analogs, could be also considered potential inhibitors of bacterial GlcN6P isomerase. If this is indeed the case, overproduction of GlmM would be expected to counteract the growth inhibition by **3**. The *E. coli* strain overexpressing the GlmM-encoding gene was constructed by transformation of the S4197 cells with the pMK3 plasmid. The transformed cells efficiently overproduced GlmM under inducing conditions, as revealed by the SDS-PAGE analysis (S13). Susceptibility of this mutant to GlcN6S was however exactly the same as that of cells carrying the empty expression plasmid pKES170 and of the wild-type cells (S13). This result clearly indicates that overproduction of GlmM does not alter bacterial susceptibility to GlcN6S, therefore this compound is unlikely to inhibit the GlmM activity.

2.5. Molecular modelling of GlcN6S and ADGS interaction with GlcN6P synthase

GlcN6P and the transition state analogs, ADGP and ADMP, are known as inhibitors of GlcN6P synthase and the crystal structures of their complexes with the bacterial or fungal enzyme were determined previously [9–11]. Looking for the structural determinants of a slightly enhanced enzyme inhibitory potential of GlcN6S and ADGS, in comparison with that of GlcN6P and ADGP, we have docked these four molecules into the active site of the isomerase domain (ISOM) of *C. albicans* GlcN6P synthase. Images of the resulting complexes are shown in Fig. 3A–D.

Phosphate oxygens of ADGP each form three hydrogen bonds with hydroxyl groups of Ser406, Ser450, Ser452 and Thr455, main chain amino groups of Ser452 and Gln451, and with water molecules tightly bound in the pocket (Fig. 3A). These water molecules can be found in very similar positions in most crystal structures of GlcN6P synthase ISOM domains available [12]. Nearly all the above specified interactions are saved in the ADGS:ISOM complex (Fig. 3B), except for the one with water. This pattern of interactions is common for many enzymes binding the phosphate group bearing ligands. The lack of the O6 oxygen atom in ADGS molecule has two consequences; namely one potential hydrogen bond acceptor is missing and the entire molecule is one atom shorter. Despite these,

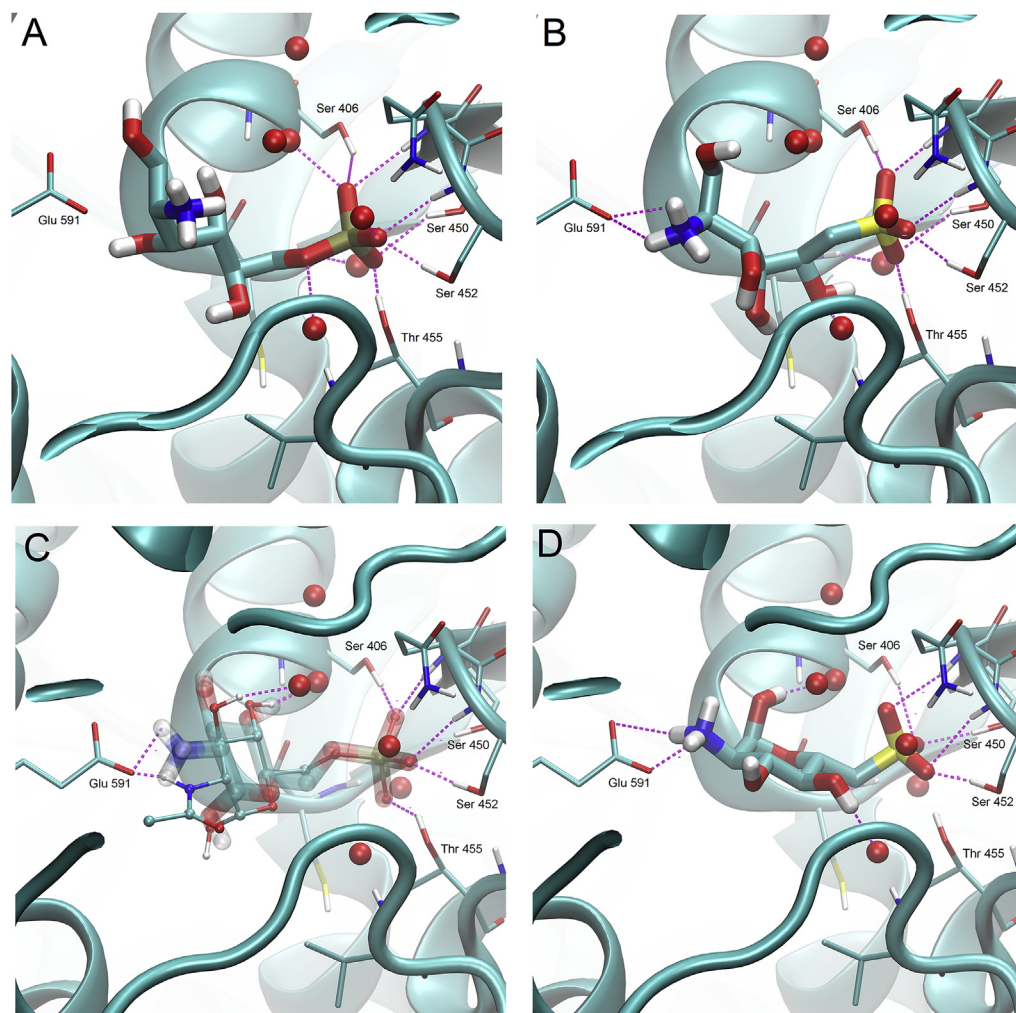


Fig. 3. Results of ligand docking to the ISOM active site. Water molecules present at the binding site are represented as red spheres. A, ADGP; B, ADGS; C, GlcN6P (transparent thick sticks) and NAcGlcN6P (thin sticks); D, GlcN6S. (For interpretation of the references to colour in this figure legend, the reader is referred to the web version of this article.)

ADGS is able to fit into the binding site in a pose resembling that of ADGP. The sulfonate group is isosteric to phosphate, except for the missing O6 atom, substituted by a methylene group. Most interactions formed by the phosphate oxygen atoms can be mimicked by corresponding sulfonate oxygens. The sulfur-bound -CH₂- moiety of ADGS (position corresponding to O6 of ADGP) is not able to form hydrogen bonds with nearby water molecules, but due to the chain shortening, the O5 hydroxyl moiety can participate in these interactions. The shortening of the aminoglucitol chain in ADGS in comparison with ADGP, results in a changed conformation of the C1–C2 part of the chain. Nevertheless, the substituents at C1 and C2 seem to be still placed in appropriate positions to mimic the respective groups in ADGP. In fact, due to the modified conformation of this part of the ADGS ligand with respect to ADGP, the N2 atom of ADGS is closer to the carboxyl of Glu591 than its counterpart in ADGP just like in the case of another GlcN6P synthase inhibitor described previously, namely ADMP [13], suggesting importance of stronger ionic interactions between the two moieties. This modification could compensate for the suboptimal pose of the remaining part of the molecule.

Similar effects have been observed for the ISOM:GlcN6S complex. This ligand, similarly to its phosphate-containing counterpart GlcN6P, was docked in the closed conformation, therefore the molecule is a bit shorter and much less flexible than the linear ADGS. Nevertheless, as shown in Fig. 3C, GlcN6S perfectly fits into the niche between Glu591 and the phosphate binding pocket, so that the ligand is firmly kept in the binding site by these two anchoring groups. Again, the strong ionic interactions between the amino group of GlcN6S and Glu591 carboxyl of ISOM compensate for the suboptimal pose of the remaining part of the molecule. Obviously these interactions must be missing when the amino group of GlcN6S is N-acetylated, moreover the N-acetyl functionality provides some steric hindrance, preventing an optimal accommodation of the ligand, so that this is not surprising that NAcGlcN6S does not inhibit the GlcN6P synthase activity. Notably, the effect of N-acetylation is less significant in the case of GlcN6P as an ISOM ligand. Since the pose of this ligand is somewhat different, its amino group is located above the Glu591 residue, so that NAcGlcN6P can be accommodated in the ISOM binding site, as shown in Fig. 3D.

3. Discussion

The 6-sulfo-6-deoxy-D-glucosamine derivatives have been designed and synthesized as potential antimicrobial agents targeting enzymes of the cytoplasmic UDP-GlcNAc pathway in human pathogenic bacteria and yeasts. The target potential of some of these enzymes has been already demonstrated, since genes encoding bacterial GlcN6P synthase GlmS [14], phosphoglucosamine mutase GlmM [15], GlcN1P acetyltransferase GlmU [16] and fungal GlcN6P synthase GFA1 [17], GlcN6P N-acetylase GNA1 [18] and NAcGlcN6P mutase AGM1 [19] have been shown to be essential. Small molecule inhibitors of GlmS/GFA1, GlmM or GlmU resulting from either rational designing or from directed screening, have been proposed and demonstrated antimicrobial activity [20,21]. Some of these compounds are structural analogs and derivatives of GlcN6P [4,21,22]. GlcN6S is also a structural analog of this amino sugar phosphate, in which the 6-phosphate functionality is replaced by sulfonate. One may therefore expect that this compound could target GlmS/GFA1 as a product analog or enzymes catalyzing the following step in the UDP-GlcNAc pathway, i.e. GlmU in bacteria or GNA1 in yeasts, as a substrate analog. In fact, Sacoman and Hollingsworth previously demonstrated an antibacterial activity of GlcN6S (complete growth inhibition of *Escherichia coli* DH5 α at 20 mg mL⁻¹) and provided evidence for inhibition of yeast

GNA1 by this compound (IC₅₀ ~ 2 mM) [6]. Our results clearly show that the primary target of GlcN6S in *E. coli* and *C. albicans* is GlcN6P synthase. Under *in vitro* conditions, *E. coli* GlmS and *C. albicans* GFA1 were effectively inhibited by GlcN6S with IC₅₀ values 0.08 mM and 0.21 mM, respectively, comparing to the IC₅₀ = 2.85 mM, found against *C. albicans* GNA1 and an apparent lack of inhibition of bacterial GlmM. Results of the molecular docking experiments confirmed effective binding of GlcN6S at the *C. albicans* GFA1 active site.

On the other hand, the anticandidal and antibacterial growth inhibitory effect of GlcN6S was observed at concentrations an order of magnitude higher than the IC₅₀s against GlmS/GFA1 determined *in vitro*, since the MIC values were 0.5–2.0 mg mL⁻¹, corresponding to 2–8 mM. This difference is most probably a consequence of slow internalization of GlcN6S by microbial cells. It should be noted however, that the phosphate-containing analogue of GlcN6S, namely GlcN6P, although known as an inhibitor of GlmS with IC₅₀ = 0.35 mM [23], does not exhibit antibacterial activity. This phenomenon may be due to the poor diffusion but possibility of a fast intracellular metabolism by phosphatases and GlcN6P deaminase NagB should be also considered. The MIC value of GlcN6S against *E. coli* found in our study (2 mg mL⁻¹) was however an order of magnitude lower than that reported previously [6], possibly due to the strain specificity and differences in growth media composition.

Antibacterial but not antifungal effect of GlcN6S was potentiated by GlcN and a dipeptide Nva-FMDP. The former is accumulated in *E. coli* cells due to the hexose phosphotransferase system manXYZ [24] that generates intracellular GlcN6P and the latter is transported by a di-tripeptide permease and cleaved intracellularly by dipeptidase to release the C-terminal FMDP [8]. In our previous studies we found that another sulfur-containing GlcN6P analog, namely D-glucosamine-6-sulfate (GlcN6SO₄), although itself devoid of antibacterial activity, potentiated that of Nva-FMDP against *E. coli* cells. That effect was due to inhibition of the GlmY/GlmZ small RNA cascade, which usually activates *glmS* expression in response to intracellular GlcN6P depletion. Upregulation of *glmS* expression overcomes Nva-FMDP-triggered inhibition of GlmS [25]. A similar mechanism may be responsible, at least in part, for the apparent antibacterial synergy of GlcN6S and Nva-FMDP, although the structural difference between GlcN6SO₄ and GlcN6S, i.e. lack of the O6 atom in the latter may affect its recognition by the GlmY/GlmZ system. Notably, the phosphonate analogs of GlcN6P effectively competed with the natural ligand in binding at the active site of *glmS* riboswitch [26], which is a metabolic regulator of *glmS* mRNA expression in gram-positive bacteria [27]. It seems however, that the major mechanism of the observed antibacterial synergy of GlcN6S and Nva-FMDP is a mutual inhibition of GlmS. Both GlcN6P and FMDP are known inhibitors of GlmS, so that one can assume a synergistic enzyme inhibition by GlcN6S/FMDP or GlcN6S/GlcN6P combinations. This is obvious in the case of the former, since FMDP and GlcN6S target different active sites of GlmS, however GlcN6S and GlcN6P compete for the same active site of the enzyme, so that the molecular basis of the latter synergy is not so clear.

Antimicrobial efficiency of GlcN6S could be slightly improved upon N-acetylation, giving rise to 2–4 times lower MIC values of NAcGlcN6S, while esterification of the sulfonate functionality resulted in loss of antibacterial and antifungal activity. Although both types of modification should enhance hydrophobicity of GlcN6S and thus facilitate free diffusion of these derivatives through the microbial cell membrane, the more important seems the possibility of enzymatic regeneration of GlcN6S in cytosol as an active inhibitor – functioning by N-deacetylation of NAcGlcN6S but not by ester hydrolysis in GlcN6SME and NAcGlcN6SME. Most likely, the *C. albicans* cells do not contain intracellular enzymes, able

to hydrolyze the sulfate or sulphonate esters. Although there are reports on existence of a fungal counterpart of mammalian enzyme, *N*-Acetylglucosamine-6-sulfate sulfatase, known also as chondroitin sulfatase [42], this is a secretory enzyme and the respective intracellular activity has never been found.

ADGS is a structural analog of a transition state *cis*-enolamine intermediate formed in the GlcN6P synthase-catalyzed reaction. Its phosphate-containing counterpart ADGP is a well-known inhibitor of GlmS and GFA1 [4,28,29]. The enzyme inhibitory potency of ADGS found in this study, was found to be a bit higher than that of ADGP but slightly lower than that of ADMP [13], which is an ADGP epimer at C-2. Results of the molecular docking of ADGS at *C. albicans* ISOM active site provided rationale for interpretation of this phenomenon by revealing a possibility of interaction of the 2-amino functionality of ADGS with Glu591 residue at the ISOM active site, unlikely to occur between ADGP and the enzyme.

NACADGS, undergoing an intracellular conversion to ADGS, exhibited the highest antimicrobial activity among the 6-sulfo-6-deoxy-D-glucosamine derivatives tested, most likely due to the facilitated diffusion through the membrane. Similar effect was previously described for *N*-acyl and *N*-alkyl derivatives of ADGP [4,30].

4. Conclusions

The 6-sulfo-6-deoxy-D-glucosamine derivatives described in this work constitute a novel group of antimicrobial agents, active against human pathogenic bacteria and yeasts. The primary molecular target of these compounds is GlcN6P synthase, catalyzing the first committed step of the UDPGlcNAc pathway. Although the antimicrobial *in vitro* activity of novel compounds is not high in terms of the MIC values, their action on bacterial or yeast cells induces cell wall destruction, as shown previously for GlcN6S acting on *Rhizobium trifolii* [6] and in this work for NACADGS acting on *Candida albicans*, so that they are bactericidal and fungicidal at 0.125–2.0 mg mL⁻¹. An interesting phenomenon is potentiation of antibacterial activity of GlcN6S by GlcN and Nva-FMDP, as one of the rare examples of synergism of two compounds targeting the same intracellular enzyme.

5. Experimental

5.1. Instrumentation and chemicals

D-Glucosamine, *N*-acetyl-D-glucosamine, sodium borohydride, triphenylphosphine, trimethoxymethane, type II L-glutamic dehydrogenase from bovine liver (GDH), 3-acetylpyridine adenine dinucleotide (APAD) and acetyl-coenzyme A (AcCoA) were purchased from Sigma-Aldrich Chemical Co. All other chemicals were of the highest purity commercially available. ¹H and ¹³C NMR spectra were obtained with Varian Unity Plus at 500 MHz. The deuterated solvents were used as an internal lock for ¹H NMR. Melting points were determined on a melting point apparatus equipped with thermometer and were uncorrected. Specific rotations were measured on a Rudolph Autopol II digital polarimeter. Column chromatography was carried out in silica gel 0.040–0.063 mm. TLC was carried out on Kieselgel 60 F₂₅₄ plates (Merck) in solvent systems: A (*n*-butanol-acetic acid-water 2:1:1 v/v/v), B (*n*-butanol-acetic acid-water 4:1:1 v/v/v), C (ethyl acetate-acetic acid-methanol 10:3:1 v/v/v). The MS analyses were carried out using the Agilent Technologies 6540 UHD Accurate-Mass Q-TOF LC/MS facility.

5.2. Syntheses

5.2.1. Benzyl 2-acetamido-D-glucopyranoside

This compound was prepared from *N*-acetyl-D-glucosamine **1** according to the method reported by Janiak et al. [4], in 54% yield; mp 181–182 °C (EtOH) (lit. mp 183–184 °C) [4]; $[\alpha]_D^{25} + 134$ (c1, EtOH) lit. $[\alpha]_D^{25} + 104$ (c1, EtOH). ¹H NMR (D₂O) δ [ppm]: 1.95 (s, 3H, CH₃CO), 3.37 (t, *J* = 9 Hz, 1H, C4), 3.66–3.72 (m, *J* = 4 and 11 Hz, 3H, C5, C3, C6'), 3.82 (dd, *J* = 10 Hz, 1H, C6), 3.88 (dt, *J* = 10 and 3 Hz, 1H, C2), 4.49 and 4.76 (AB, 2 × d, 2H, CH₂-Ph), 4.87 (d, *J* = 4 Hz, 1H, C1), 7.27–7.39 (m, 5H, C₆H₅).

5.2.2. Benzyl 2-acetamido-6-bromo-2,6-dideoxy-D-glucopyranoside

Benzyl 2-acetamido-D-glucopyranoside (4.5 g, 14.45 mmol) and tetrabromomethane (9.6 g, 28.94 mmol) were added to the ice-cold, stirred solution of 15.1 g (57.19 mmol) triphenylphosphine in pyridine (180 mL). The reaction mixture was stirred under reflux (60–65 °C) for 45 min. The solvent was evaporated *in vacuo* and the residue was treated with toluene (3 × 70 mL). The mixture was shaken vigorously and the organic layer was separated. The crude product was purified by column chromatography on silica gel eluted with chloroform and chloroform:metanol 30:1 v/v. The final product was crystallised from chloroform as white needles: 3.52 g (yield 65%) mp 178–179 °C (lit. mp 184–185 °C); $[\alpha]_D^{25} + 175$ (c1, MeOH) lit. $[\alpha]_D^{25} + 100$ (c1, MeOH) [31]. ¹H NMR (CD₃OD) δ [ppm]: 1.82 (s, 3H, CH₃CO), 3.15 (q, *J* = 11 Hz, 1H, C2), 3.61 and 3.63 (m, 2H, C6), 3.64 (d, *J* = 9 Hz, 1H, C5), 4.45 (d, *J* = 12 Hz, 1H, C4), 4.67 (d, *J* = 12 Hz, 1H, C3), 4.70 (AB, 2H, CH₂-Ph), 4.73 (d, *J* = 4 Hz, 1H, C1), 4.89 (d, *J* = 6 Hz, 1H, C3-OH), 5.37 (d, *J* = 6 Hz, 1H, C4-OH) 7.27–7.39 (m, 5H, C₆H₅), 7.88 (d, *J* = 8 Hz, 1H, NH). MS-ESI: *m/z* calcd. for C₁₅H₂₀BrNO₅: 374.2270; found 374.2573 [M]⁺; 376.2573 [M+2]⁺.

5.2.3. Benzyl 2-acetamido-2,6-dideoxy-6-sulfo-D-glucopyranoside **2**

The magnetically stirred solution of benzyl 2-acetamido-6-bromo-2,6-dideoxy-D-glucopyranoside **3** (400 mg, 1.07 mmol) in 6 mL of water was heated (80 °C) for 3 h Na₂SO₃ powder (500 mg, 3.97 mmol) was added to the resulting mixture and heating was continued for 4 h. The mixture was concentrated by evaporation and purified by chromatography on Amberlite IRA 400 (OH⁻) eluted with 3% aq. HCl, to give the product as a pale yellow oil, with 43% yield (170 mg). R_f(C) 0.12. ¹H NMR (D₂O) δ [ppm]: 1.76 (s, 3H, CH₃CO), 2.94 (dd, *J* = 10 and 14.6 Hz, 1H, C2), 3.13 (m, *J* = 11.7 and 7 Hz, 2H, C6), 3.22 (d, *J* = 14 Hz, 1H, C5), 3.54 (m, *J* = 8.8 and 4.4 Hz, 1H, C4), 3.70 and 4.68 (AB, *J* = 4 Hz, 2H, CH₂Ph), 4.01 (t, *J* = 19 Hz, 1H, C3), 4.31 (d, *J* = 11 Hz, 1H, C1), 7.19–7.26 (m, 5H, C₆H₅). MS-ESI: *m/z* calcd. for C₁₅H₂₁NSO₈: 375.3941; found 376.4084 [M+1]⁺.

5.2.4. 2-Amino-2,6-dideoxy-6-sulfo-D-glucopyranose **3**

The magnetically stirred solution of benzyl 2-acetamido-2,6-dideoxy-6-sulfo-D-glucopyranoside (500 mg, 1.33 mmol) in 4 mL 36% HCl:water (1:1 v/v) mixture was heated under reflux for 6 h. The resulting mixture was evaporated *in vacuo*. The residue was dissolved in water and purified by chromatography on the Amberlite IRA 400 (OH⁻) eluted with 3% aq. HCl, to give the product **3** as a white solid, with 60% yield (194 mg). R_f(A) 0.24. The equilibrium mixture contained two anomers $\alpha:\beta = 4:1$. ¹H NMR (D₂O) δ [ppm]: 2.84 (t, 1H, C6'β), 2.9 (dd, *J* = 10 Hz, 1H, C2β), 2.91 (dd, *J* = 9.8 and 14.7 Hz, 1H, C6'α), 3.12–3.20 (m, 4H, C4α, C6β, C2α, C4β), 3.25 (d, *J* = 1.7 and 14.7 Hz, 1H, C6α), 3.55 (t, *J* = 9 Hz, 1H, C5β), 3.68 (t, *J* = 9 Hz, 1H, C3β), 3.72 (t, *J* = 9.4 Hz, 1H, C3α), 4.10 (t, *J* = 9.8 Hz, 1H, C5α), 4.76 (d, *J* = 8 Hz, 1H, C1β), 5.23 (d, *J* = 3.4 Hz, 1H, C1α). ¹³C NMR (D₂O) δ [ppm]: 89.18, 72.54, 69.63, 67.98, 54.30, 52.05. MS-ESI: *m/z* calcd. for C₆H₁₃NSO₇: 243.0413; found 244.0400 [M+1]⁺.

5.2.5. Methyl 2-amino-2,6-dideoxy-D-glucopyranose-6-sulfonate 4

2-amino-2,6-dideoxy-6-sulfo-D-glucopyranose **3** (200 mg, 0.82 mmol) was suspended in 5 mL of methanol and 2 mL of trimethoxymethane was added. After 24 h, the mixture was purified by preparative TLC chromatography using as an eluent the *n*-BuOH:AcOH:H₂O 4:1:1 v/v system. The product was obtained as a yellow oil, with 30% yield (64 mg). *R_f* (B) 0.37. The equilibrium mixture contained two anomers $\alpha:\beta = 1:4$. ¹H NMR (D₂O:CD₃OD) δ [ppm]: 2.95 (m, 1H, C'6), 3.35 (s, 3H, SO₃CH₃), 3.4–3.6 (m, 3H, C6, C4, C2), 3.95 (t, 1H, C5), 4.10 (t, 1H, C3), 5.10 (d, *J* = 3.4 Hz, 1H, C1). MS-ESI: *m/z* calcd. for C₈H₁₅NSO₈: 257.0569; found 258.0721 [M+1]⁺.

5.2.6. 2-amino-2-deoxy-D-glucitol-6-sulphonic acid 5

2-amino-2,6-dideoxy-6-sulfo-D-glucopyranose **3** (850 mg, 3.49 mmol) was dissolved in 15 mL of ethanol and cooled on ice for 10 min. Sodium borohydride (250 mg, 6.61 mmol) was added to the mixture in small portions over 10 min. The solution obtained was stirred for 3 h at room temperature. After this time, the mixture was cooled on ice again and another portion of NaBH₄ (150 mg, 3.97 mmol) was added. Reaction was completed after 12 h. The mixture was filtrated and solution was applied to a Amberlite IRA 400 resin, OH⁻ form. The product was eluted with 0.25 M HCl, with 96% yield (823 mg). *R_f* (A) 0.10. ¹H NMR (D₂O) δ [ppm]: 2.9 (m, 1H), 3.28 (m, 2H), 3.4 (q, 2H), 3.6 (m, 1H), 3.8 (m, 2H). MS-ESI: *m/z* calcd. for C₆H₁₅NSO₇: 245.0596; found 246.0601 [M+1]⁺.

5.2.7. 2-Acetamido-2,6-dideoxy-6-sulfo-D-glucopyranose 6

Benzyl 2-acetamido-2,6-dideoxy-6-sulfo-D-glucopyranoside **2** (500 mg, 1.33 mmol) was dissolved in 95% ethanol (5 mL) and 20 mg of Pd/C (10%) was added. The resulting mixture was stirred under hydrogen pressure for 18 h. Subsequently, Pd/C was filtered off and the residual solvent was removed by evaporation. The mixture was purified by TLC chromatography using the solvent system B as an eluent. The product **6** was obtained as a yellow oil, with 70% yield (267 mg). *R_f* (B) 0.31. The equilibrium mixture contained two anomers $\alpha:\beta = 1:4$. ¹H NMR (D₂O:CD₃OD) for anomer β δ [ppm]: 1.85 (s, 3H, CH₃CO), 2.95 (m, 1H), 3.10 (m, 1H), 3.5 (dd, 1H), 3.6–3.7 (m, 2H), 4.5 (d, *J* = 8 Hz, 1H, C1). ¹³C NMR (D₂O) δ [ppm]: 97.8, 73.7, 67.9, 55.3, 53.9, 52.1, 22.2. ¹³C NMR (D₂O) δ [ppm]: 97.79 C1, 73.69 C4, 67.90 C3, 55.31 C5, 53.94 C2, 52.08 C6, 22.17 CH₃. MS-ESI: *m/z* calcd. for C₈H₁₅NSO₈: 285.2716; found 284.2623 [M-1]⁻.

5.2.8. Methyl 2-acetamido-2,6-dideoxy-D-glucopyranose-6-sulfonate 7

2-acetamido-2,6-dideoxy-6-sulfo-D-glucopyranose **6** (200 mg, 0.7 mmol) was suspended in 5 mL of methanol and 2 mL of trimethoxymethane was added. After 24 h, the mixture was purified by TLC chromatography using the solvent system B as an eluent. The product was obtained as a yellow oil, with 35% yield (73 mg). *R_f* (B) 0.41. The equilibrium mixture contained two anomers $\alpha:\beta = 1:8$. ¹H NMR (D₂O) for anomer β δ [ppm]: 1.75 (s, 3H, CH₃CO), 3.13 (m, 3H), 3.3–3.4 (m, 3H), 3.5 (s, 3H, SO₃CH₃), 4.5 (d, 1H, C1). MS-ESI: *m/z* calcd. for C₉H₁₇NSO₈: 299.0675; found 298.0602 [M-1]⁻.

5.2.9. N-acetyl-2-amino-2-deoxy-D-glucitol-6-sulphonic acid 8

N-acetyl-2-amino-2,6-dideoxy-6-sulfo-D-glucopyranose **6** (900 mg, 3.15 mmol) was dissolved in 15 mL of ethanol and cooled on ice for 10 min. Sodium borohydride (300 mg, 7.93 mmol) was added to the mixture in small portions over 10 min. The solution obtained was stirred for 3 h at room temperature. After this time, the mixture was cooled on ice again and another portion of NaBH₄ (150 mg, 3.97 mmol) was added. The reaction was completed after 12 h. The mixture was filtrated and solution was applied to a

Amberlite IRA 400 resin, OH⁻ form. Product was eluted with 0.25 M HCl, with 94% yield (850 mg). *R_f* (A) 0.14. ¹H NMR (D₂O) δ [ppm]: 1.75 (s, 3H), 2.8 (m, 1H), 3.20 (m, 1H), 3.3 (m, 1H), 3.4 (m, 1H), 3.5–3.7 (m, 2H), 3.7 (m, 1H), 3.9 (m, 1H). MS-ESI: *m/z* calcd. for C₈H₁₇NSO₈: 287.067; found 288.0754 [M+1]⁺.

5.3. Microorganisms and growth conditions

Antimicrobial activity was tested against *Candida albicans* ATCC 10231, *Candida glabrata* DSM 11226, *Candida arborea* KKP 319, *Candida krusei* DSM 6128, *Staphylococcus aureus* PCM 2051, *Staphylococcus epidermidis* PCM 2118, *Escherichia coli* K12 and *Pseudomonas aeruginosa* ATCC 27853 strains. Yeast cells were routinely grown in Sabouraud medium at 30 °C and bacteria in Mueller-Hinton Broth at 37 °C.

5.4. Determination of antimicrobial in vitro activity

MIC values of tested compounds were determined by the serial dilution microplate methods. Susceptibility of yeasts from the *Candida* genus was assayed in the RPMI-1640 medium by the slightly modified method recommended by CLSI [32]. Turbidity in individual wells was measured with a microplate reader (Victor³V, PerkinElmer). The MIC was defined as the lowest drug concentration at which at least 80% decrease in turbidity, in comparison to the drug-free control, was observed. Susceptibility of bacteria was assayed in the Mueller-Hinton Broth medium according to the standardized procedure [33].

Disk diffusion assays were carried out on McConkey lactose (bacteria) or Sabouraud (yeasts) agar plates. Cells were grown at 37 °C in LB to an OD₆₀₀ ~ 0.5, pelleted and re-suspended in the medium subsequently used in the assay. A volume containing ~4 × 10⁷ cells was mixed with 4 mL thin agar layer (medium containing 7.5% agarose) that was kept molten at 44 °C and subsequently spread over 15 mL solid agar base of the same medium prepared in 100 mm Petri dishes. The compounds to be tested were adsorbed onto 6 mm cellulose disks, which were subsequently placed on the seeded agar surface in the Petri dishes. Growth inhibition zones were recorded following incubation for 16 h at 37 °C. Assays were performed at least twice using independent cultures.

Methods for preparation of *C. albicans* cell-free extract and for purification of *C. albicans* GlcN6P synthase to near homogeneity, were described previously [34]. Cell-free extract of *E. coli* NK7356(pGM10) cells containing overproduced GlcN6P synthase was prepared as described [35].

5.5. Construction and analysis of an *E. coli* strain overexpressing *glmM*

To assess the effect of *GlmM* overproduction on drug susceptibility in *E. coli*, plasmid pMK3 was constructed, which allows for IPTG-inducible expression of *glmM*. The *glmM* gene was amplified by PCR using oligonucleotides BG1284 (5'-GAAGTACCATGGA-GATCTTAATAATTTTGTAACTTTAAGAAGGAGATATACA-TATGAGTAATCGTAAATATTTTC) and BG1285 (5'-GGCCTGCAGTTAAACGGCTTTTACTGC). Forward primer BG1284 introduced the Shine-Dalgarno sequence from phage T7 *gene10* upstream of *glmM* to achieve strong translation rates. The PCR fragment was digested with NcoI and PstI and inserted between the same sites downstream of the *P_{tac}* promoter on plasmid pKES170 [36]. Plasmid pMK3 and for comparison the empty expression vector pKES170 were introduced into *E. coli*-K12 strain S4197, which is a $\Delta lacZ$ derivative of the widely used MG1655 reference strain [37]. To check for *glmM* overexpression, strain S4197 carrying plasmid pKES170 or pMK3 was grown at 37 °C in LB medium

containing 100 µg/mL ampicillin. 1 mM IPTG was added, when the cultures reached an OD₆₀₀ of 0.8 and growth was continued for 1 h. Cells were harvested and extracts corresponding to 3.25 µg total protein, respectively, were separated on denaturing SDS polyacrylamide gels, which were subsequently stained with Coomassie blue. Disc diffusion assays using the *glmM* overproducing strain were carried out as described, but as a difference plates were supplemented with 100 µg/mL ampicillin and with 1 mM IPTG where indicated.

5.6. Enzyme activity assays

GlcN6P synthase. Enzyme activity was measured by two methods: a) quantification GlcN6P formed or b) quantification of L-glutamate formed. Method A: Reactions were carried out in mixture containing 25 mM phosphate buffer, pH 7.0, 1 mM EDTA, 1 mM DTT, 7.5 mM D-Fru6P, 10 mM L-glutamine, GlcN6P synthase (0.1–0.2 µg) and a given inhibitor at appropriate concentration in the 0–5 mM range. The reaction was carried out at 30 °C for 30 min and stopped by heating. Concentration of GlcN6P formed was determined by the modified Elson-Morgan method [38]. Method B: Reactions were carried out in 2 mL of mixtures containing 25 mM phosphate buffer, pH 7.0, containing 1 mM EDTA, 1 mM DTT, 7.5 mM D-Fru6P, 10 mM L-glutamine, 0.3 mM APAD, GDH (30 units mL⁻¹) and a given inhibitor at appropriate concentration in the 0–5 mM range. The mixtures were incubated at 30 °C. Absorbance at 365 nm was measured until equilibrium, GlcN6P synthase preparation (0.1–0.2 µg in 5 µL) was added and A₃₆₅ measurement was continued. Increase of A₃₆₅ was linear for at least 15 min. The enzyme activity was calculated by assuming $\epsilon_{365}(\text{APAD}) = 0.91 \text{ L} \times \text{mm}^{-1} \times \text{mmol}^{-1}$ [39].

GlcN6P N-acetylase. Enzyme activity was assayed in solution containing 50 mM Tris-HCl buffer pH 7.5, 150 µM GlcN6P, 150 µM AcCoA, 5 mM MgCl₂, appropriately diluted *C. albicans* cell-free extract and an enzyme inhibitor at appropriate concentration. The reaction was carried out at 30 °C for 30 min and stopped by heating. Concentration of the CoA formed was determined with 2-nitrobenzoic acid, as described previously [18].

The IC₅₀ values were read from the enzyme activity = f(inhibitor concentration) curves.

5.7. Monitoring morphological changes

C. albicans ATCC 10231 cells from the overnight cultures in Sabouraud medium were harvested, washed with sterile saline and suspended in RPMI 1640 medium to the final cell density of 10⁵ cfu mL⁻¹. Tested compounds were added at appropriate concentrations and cultures were incubated for 6 h at 30 °C, with shaking. At time intervals, samples of 0.1 mL were collected and cells were stained for chitin. The culture sample was combined with 0.1 mL of the Calcofluor White solution (0.3 mg mL⁻¹ in 25 mM phosphate-buffered saline/PBS/, pH 7.0) and incubated for 5 min at 25 °C. The cells were then harvested, washed four times with PBS, re-suspended in 0.1 mL of the fresh PBS and transferred to a microscopic slide. The stained cells were examined with the Olympus BX 60 F5 fluorescence microscope and photographs were taken using the Studio Lite software (Pixera Corporation, USA).

5.8. Investigation of metabolism of novel compounds in a cell-free extract of *C. albicans* cells

A concentrated solution of compound **4**, **6**, **7** or **8** was added to the cell-free extract, prepared from *C. albicans* ATCC 10231 cells, to give a final concentration of 5 mg mL⁻¹. The mixture was incubated at 30 °C. Samples of 1 mL were collected at hourly intervals and

proteins were precipitated by addition of 1 mL of ethanol. The protein precipitate was removed by filtration and the composition of the filtrate was determined by TLC analysis of the filtrates (solvent system A).

5.9. Molecular modelling

Model of the receptor used for docking was based on the structure of *C. albicans* GlcN6P synthase ISOM domain in complex with 2-amino-2-deoxy-D-mannitol-6-phosphate (ADMP) and UDP-GlcNAc, available in PDB (pdbid: 2poc) [11]. Missing or incomplete residues were homology modeled by means of the MODELLER9v2 package [40], using as a template structure of the bacterial GlcN6P synthase (pdbid: 1jxa). Water molecules, known to play an important role in GlcN6P synthase ISOM active site by bridging the interactions between a ligand and the protein, were kept as a part of the model.

The Autodock 4.2 software [41] and its utility scripts were used for both ligand and receptor preparation, as well as for all docking calculations. Grid maps were centered at the center of the binding site and their dimensions were set to 70 steps in each direction (with default grid step size), so that the entire binding pocket was covered. The Lamarckian genetic algorithm was used as a search protocol. The maximum number of energy evaluations was set to 25,000,000 and the maximum number of generations to 27,000. The receptor was kept rigid while the ligands were flexible during docking. For each ligand, 50 independent runs were performed and the resulting poses were clustered with the tolerance of 2 Å. Ligand poses from the most abundant low energy clusters were selected for analysis.

To verify the reliability of the docking protocol, the ADGP molecule was docked first into the ISOM active site and its resulting pose was compared to a ligand pose found in the crystal structure of bacterial GlcN6P synthase:ADGP complex (1mos) [10]. Similarly, a pose of GlcN6P docked into the ISOM active site was compared to a ligand pose found in the crystal structure of bacterial GlcN6P synthase:GlcN6P complex (1moq) [9].

Declaration of interest

The authors declare no conflict of interest.

Acknowledgements

This work was supported in part by the UMO-2014/13/B/NZ7/02305 grant from the Polish National Science Centre to MJM and by the 'Austrian Science Fund' (FWF) [grant number P 26681-B22 to BG].

References

- [1] S. Milewski, I. Gabriel, J. Olchowoy, *Yeast* 23 (2006) 1–14.
- [2] L.L. Silver, *Ann. N. Y. Acad. Sci.* 1277 (2013) 29–53.
- [3] S. Milewski, *Biochim. Biophys. Acta* 1597 (2002) 173–192.
- [4] A. Janiak, M. Hoffmann, M.J. Milewska, S. Milewski, *Bioorg. Med. Chem.* 11 (2003) 1653–1662.
- [5] L.I. Alvarez-Anorve, I. Gaugue, H. Link, et al., *J. Bacteriol.* 198 (2016) 1610–1620.
- [6] J.L. Sacoman, R.I. Hollingsworth, *Carbohydr. Res.* 346 (2011) 2294–2299.
- [7] R. Andruszkiewicz, H. Chmara, S. Milewski, E. Borowski, *J. Med. Chem.* 30 (1987) 1715–1719.
- [8] H. Chmara, S. Milewski, R. Andruszkiewicz, F. Mignini, E. Borowski, *Microbiology-UK* 144 (1998) 1349–1358.
- [9] A. Teplyakov, G. Obmolova, M.-A. Badet-Denisot, B. Badet, I. Polikarpov, *Structure* 6 (1998) 1047–1055.
- [10] A. Teplyakov, G. Obmolova, M.-A. Badet-Denisot, B. Badet, *Protein Sci.* 8 (1999) 596–602.
- [11] J. Raczynska, J. Olchowoy, P.V. Konariyev, D.I. Svergun, S. Milewski, W. Rypniewski, *J. Mol. Biol.* 372 (2007) 672–688.

- [12] N. Floquet, C. Richez, P. Durand, B. Maigret, B. Badet, M.-A. Badet-Denisot, *Bioorg Med. Chem. Lett.* 17 (2007) 1966–1970.
- [13] S. Milewski, A. Janiak, M. Wojciechowski, *Arch. Biochem. Biophys.* 450 (2006) 39–49.
- [14] M. Sarvas, *J. Bacteriol.* 105 (1971) 467–471.
- [15] D. Mengin-Lecreux, J. van Heijenoort, *J. Biol. Chem.* 271 (1996) 32–39.
- [16] E.T. Buurman, B. Andrews, N. Gao, *J. Biol. Chem.* 286 (2011) 40734–40742.
- [17] W.L. Whelan, C.E. Ballou, *J. Bacteriol.* 124 (1975) 1545–1557.
- [18] T. Mio, M. Kokado, M. Arisawa, H. Yamada-Okabe, *Microbiology-UK* 146 (2000) 1753–1758.
- [19] W. Fang, T. Du, O.G. Raimi, et al., *Biosci. Rep.* 33 (2013) 689–699.
- [20] S.S. Stokes, R. Albert, E.T. Buurman, et al., *Bioorg Med. Chem. Lett.* 22 (2012) 1510–1519.
- [21] Y. Li, Y. Zhou, Y. Ma, X. Li, *Carbohydr. Res.* 346 (2011) 1714–1720.
- [22] R. Sharma, C. Rani, R. Mehra, et al., *Appl. Microbiol. Biotechnol.* 100 (2016) 3071–3085.
- [23] B. Badet, P. Vermoote, F. Le Goffic, *Biochemistry* 27 (1988) 2282–2287.
- [24] M.C. Jones-Mortimer, H.L. Kornberg, *J. Gen. Microbiol.* 117 (1980) 369–376.
- [25] M.A. Khan, Y. Göpel, S. Milewski, B. Görke, *Front. Microbiol.* 7 (2016). Article Number 908.
- [26] X. Fei, T. Holmes, J. Diddle, et al., *ACS Chem. Biol.* 9 (2014) 2875–2882.
- [27] W.C. Winkler, A. Nahvi, A. Roth, J.A. Collins, R.R. Breaker, *Nature* 428 (2004) 281–286.
- [28] M.-A. Badet-Denisot, C. Leriche, F. Massiere, B. Badet, *Bioorg Med. Chem. Lett.* 5 (1995) 815–820.
- [29] S.L. Bearne, C. Blouin, *J. Biol. Chem.* 275 (2000) 135–140.
- [30] A. Melcer, I. Łącka, I. Gabriel, et al., *Bioorg Med. Chem. Lett.* 17 (2007) 6602–6606.
- [31] R.A. Gallemmo, D. Horton, *Carbohydr. Res.* 119 (1983) 231–240.
- [32] Clinical Laboratory Standards Institute, Reference Method for Broth Dilution Antifungal Susceptibility Testing of Yeasts, second ed., CLSI, Wayne, PA, 2008. Approved Standard M27–A3.
- [33] Clinical Laboratory Standards Institute, Methods for Dilution Antimicrobial Susceptibility Tests for Bacteria that Grow Aerobically, CLSI, Wayne, PA, 2009. Approved standard M07–A8.
- [34] S. Milewski, D. Kuszczak, R. Jędrzejczak, R.J. Smith, A.J.P. Brown, G.W. Gooday, *J. Biol. Chem.* 274 (1999) 4000–4008.
- [35] S. Dutka-Malen, P. Mazodier, B. Badet, *Biochimie* 70 (1988) 287–290.
- [36] D. Lüttmann, R. Heermann, B. Zimmer, et al., *Mol. Microbiol.* 72 (2009) 978–994.
- [37] G.R. Venkatesh, F.C. Kembou Koungni, A. Paukner, T. Stratmann, B. Blissenbach, K. Schnetz, *J. Bacteriol.* 192 (2010) 6456–6464.
- [38] M. Kenig, E. Vandamme, E.P. Abraham, *J. Gen. Microbiol.* 94 (1976) 46–54.
- [39] H.O. Beutler, M. Supp, in: H.U. Bergmeyer (Ed.), *Methods of Enzymatic Analysis*, vol 11, Verlag Chemie, Weinheim, 1983, pp. 331–335.
- [40] A. Sali, T. Blundell, *J. Mol. Biol.* 234 (1993) 779–815.
- [41] G. Morris, R. Huey, W. Lindstrom, et al., *J. Comput. Chem.* 30 (2009) 2785–2791.
- [42] M.T. Shimizu, N.Q. Almeida, V. Fantinato, C.S. Uriterkircher, *Mycoses* 39 (1996) 161–167.

